Nucleic Acids Research, 2004, Vol. 32, No. 10 ***e83***
DOI: 10.1093/nar/gnh080

A high-throughput assay for Tn*5* Tnp-induced DNA cleavage

Brandon Ason and William S. Reznikoff*

Department of Biochemistry, University of Wisconsin-Madison, 433 Babcock Drive, Madison, WI 53706, USA

Received March 24, 2004; Revised April 22, 2004; Accepted May 15, 2004

ABSTRACT

Transposition causes genomic instability by mobilizing DNA elements. This phenomenon is mechanistically related to other DNA rearrangements, such as V(D)J recombination and retroviral DNA integration. A conserved active site architecture within the transposase/integrase superfamily catalyzes these distinct phenomena. The Tn*5* transposase (Tnp) falls within this protein class, and many intermediates of the Tn*5* transposition reaction have been characterized. Here, we describe a method for the rapid identification of Tn*5* Tnp small molecule effectors. This high-throughput screening strategy will aid in the identification of compounds that perturb Tnp-induced DNA cleavage. This method is advantageous, since it identifies effectors that specifically inhibit catalysis without inhibiting Tnp–DNA binding interactions. Effectors identified using this method will serve as a valuable aid both in the isolation and characterization of metal-bound reaction intermediates and in co-crystallization studies involving the effector, Tnp and DNA, to identify the structural basis of the interaction. Furthermore, since Tn*5* Tnp shares a similar active site architecture to other transposase/integrase superfamily members, this strategy and any effectors identified using this method will be readily applicable to these other systems.

INTRODUCTION

A variety of mechanisms for mobilizing DNA elements have evolved, differing both in the number of proteins and in the mechanism required to carry out these rearrangements (1). The cleavage mechanism can range from double-strand breaks, in the case of Tn*5*, to strand nicking and 3′ end processing. Although the nature of strand cleavage varies, all members of the transposase/integrase superfamily use a conserved active site geometry to carry out these DNA processing reactions (2–9). The catalytic core within this protein family contains three acidic amino acid residues, known as the DDE motif (10). The spatial location of these residues within the active site of each protein is surprisingly close to one another, as observed by the overlay of the Tn*5* transposase (Tnp) and ASV integrase structures (11).

The DDE residues are responsible for the divalent metal coordination required for catalysis. These residues generate nucleophilic water molecules within the active site that nick the DNA strand. In the case of Tn*5* Tnp, the 3′ hydroxyl group generated by the initial nick in turn acts as the nucleophile to attack the complementary DNA strand generating a hairpin. The DNA hairpin is subsequently resolved through an attack by an additional activated water molecule to form a double-strand break in the DNA releasing the transposon from the donor site. Following strand cleavage, the two Tnp proteins tether the transposon end sequences to a third DNA molecule containing a target site for transposon insertion. Strand transfer subsequently occurs, and, in the case of Tn*5*, generates a 9 bp duplication, which flanks the newly inserted transposon (12).

Mechanistic probes would serve as a useful tool to probe many of these reaction intermediates, as conformational differences exist between Tnp–DNA intermediates and presumably metal bound and free complexes (6,11,13,14). Here, we describe a method for the rapid identification of Tn*5* Tnp strand cleavage effectors. This method is based on the change in fluorescence polarization (FP) of a selectively labeled DNA fragment. In this assay, a change in FP accompanies the release of the labeled DNA fragment following strand cleavage. This method is readily transferable to robotic manipulation, since there are no wash steps, only a limited the number of fluid transfer steps, and requires a minimal sample volume. In addition, this assay is well suited for use in studying other transposase/integrase systems, such as HIV-1 integration or RAG-mediated V(D)J cleavage. Thus, effectors identified using this method may serve both as mechanistic probes and as potential leads in drug discovery.

MATERIALS AND METHODS

DNA substrates

The short oligonucleotides used for these experiments were purchased from Integrated DNA Technology (IDT). The short oligonucleotides were annealed to form double-stranded DNA (dsDNA) by adding 2 μmol of each oligonucleotide to a 20 mM Tris–HCl, pH 7.9, 10 mM NaCl solution for a 2 μM final oligonucleotide concentration. To anneal the single-stranded DNA (ssDNA), the oligonucleotides were heated at 96°C for 1 min followed by a decrease in temperature at the rate of 0.1°C/s to 4°C. The transferred strand is labeled with rhodamine green for the FP assays or fluorescein for native

*To whom correspondence should be addressed. Tel: +1 608 262 3608; Fax: +1 608 262 3453; Email: reznikoff@biochem.wisc.edu

gel-shift assays. Fluorescent oligonucleotides were purifed using high-performance liquid chromatography and were obtained from IDT.

The sequences of the 50 nt DNA fragments used for FP assays are 5′-TGCAGGTCGACTGTCTCTTATACACATC-TTGAGTGAGTGAGCATGCATGT-3′ and its complement. The dsDNA produced from these two fragments consists of 10 bp of donor and 40 bp of transposon DNA. Only the 5′ end of the non-transferred strand is fluorescently labeled for the experiments using this dsDNA substrate. The sequences of the 60 nt DNA fragments used for the gel-shift assays are 5′-GGCCACGACACGCTCCCGCGCTGTCTCTTATACACAT-CTTGAGTGAGTGAGCATGCAGT-3′ and its complement. The dsDNA produced from these two fragments consists of 20 bp of donor and 40 bp of transposon DNA, which are both labeled with fluorescein on their 5′ ends.

Transposase purification

The EK54, MA56 and LP372 hyperactive mutant version of Tnp is used for all assays and will be referred to as Tnp throughout this paper. Tnp was purified as described previously (15). All Tnp protein preparations were quantified using a Bradford assay with BSA as the standard.

Strand cleavage assays

In these assays, two DNA fragments each containing the Tnp recognition sequence were used to mimic the Tn*5* transposon. The cleavage reactions were carried out by incubating 800 nM Tnp with 160 nM dsDNA at 37°C for 1.5 h in cleavage buffer (25 mM Hepes, pH 7.5, 2 mM Tris–HCl pH 7.5, 100 mM potassium glutamate, 9 mM NaCl, 0.5 mM 2-mercaptoethanol, 10 μg/ml t-RNA, 0.25 mg/ml BSA, 9% glycerol and 10 mM magnesium acetate). For FP analysis, the 60 μl reactions were analyzed using the FP protocol on a Wallac Victor V plate reader with the instruments fluorescein filters, F485 excitation and F535 emission. The readings were taken 8 mm from the bottom of the plate with the G factor set at 1 and a 0.1 s counting time. The polarization aperture is set at 'normal' and the CW-lamp energy is set at the maximum, 65 535.

For gel-shift assays, after incubation at 37°C, a 20 μl aliquot of each reaction is mixed with 6 μl of 6× loading dye (Promega) and electrophoresed on either 9 or 10% native polyacrylamide gel at 300 V. After 3 h, the gel is scanned using a FluorImager SI (Vistra Fluorescence), and the bands are quantified using Image Quant (Molecular Dynamics). Increasing concentrations of EDTA (0, 0.01, 0.05, 0.1, 0.5, 1, 2, 3, 4, 5, 10, 20, 50 M) were used as a metal chelator during assay development, since strand cleavage is metal dependent.

RESULTS AND DISCUSSION

Development of a high-throughput screen for Tn*5* Tnp-induced strand cleavage

This assay was developed to screening for small molecules that specifically inhibit Tnp cleavage activity. Our method is based on the change in polarization of a fluorescently tagged dsDNA fragment. In general, FP measures the tumbling rate of a population of fluorescently labeled molecules between the time of fluorophore excitation and emission. For this assay, we used short fluorescently labeled dsDNA fragments each containing one Tnp recognition sequence. These dsDNA fragments are selectively labeled on the donor DNA end, the 5′ end of the non-transferred strand (Figure 1A). Following strand cleavage, the donor fragment is released. Thus, as the population of cleaved DNA fragments increases, the FP value decreases, because the shorter labeled DNA fragments exhibit a faster tumbling rate in solution (Figure 1B).

A comparison of these FP and gel-shift assay data reveal that the two assays are in good agreement with one another (Figure 2). In these experiments, increasing concentrations of EDTA were added to the reactions to inhibit catalysis. Thus, the change in FP represents a shift in the population towards more Tnp–DNA complexes compared to free cleaved DNA fragments in solution. In gel-shift assays, inhibition of strand cleavage corresponds to an increase in signal for the band corresponding to Tnp–DNA complexes paralleled by a decrease in the band corresponding to the cleaved DNA product. Comparing Figure 2A and B reveals that the same concentration of EDTA inhibits strand cleavage in both the FP and gel-shift assays suggesting that under these conditions FP is a good measurement of the degree of strand cleavage. Furthermore, this FP assay has a z′-value of 0.57, under these conditions, indicating that the assay window and precision are sufficient for high-throughput screening (16).

It is worth noting that the order of addition of the DNA, transposase and potential inhibitor are not critical for distinguishing between inhibitors of complex assembly and cleavage. Instead, one simply needs to compare each test reaction to the average value obtained for the entire screen, which eliminates the need to take multiple measurements per sample test reaction. The average sample value typically lies near the value for an uninhibited reaction, since most compounds in a random screen would not have an effect on the reaction.

Potential applications

Here, we present the development of a high-throughput screen to identify compounds that inhibit Tn*5* Tnp-induced strand cleavage. This technique will be useful for identifying compounds that specifically inhibit catalysis, since the free DNA substrate and the cleaved donor DNA tumble relatively quickly compared with the Tnp–DNA complex (Figure 3). Thus, compounds that directly inhibit catalysis can be distinguished from inhibitors of complex assembly. This method, in fact, increases the specificity for strand cleavage and reduces the population of hits produced from library screening, since any compound that inhibits complex assembly would exhibit a similar FP value to the uninhibited reaction. The elimination of compounds that inhibit Tnp–DNA binding is advantageous, since this should reduce the number of promiscuous inhibitors that are identified as hits, focusing the screen on compounds that specifically inhibit catalysis.

Compounds identified from this screen could be used to trap intermediates of the reaction. Previous data suggest that conformational differences exist between different Tnp–DNA intermediates as well as metal-bound and free complexes for this protein superfamily (13,17–23). Effectors identified using this screen would be particularly useful in examining

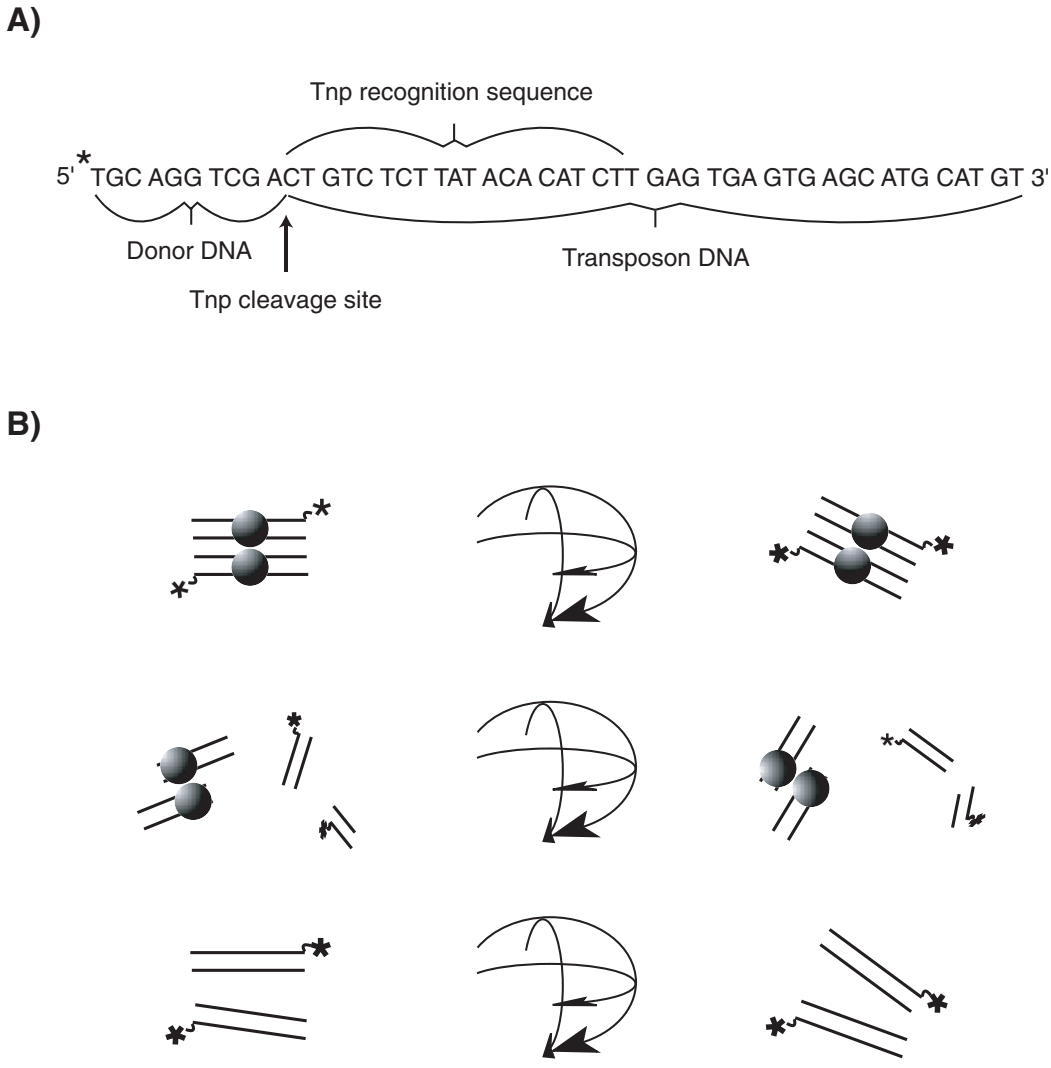

Figure 1. A schematic representation of the fluorescently labeled non-transferred DNA strand and the FP assay. (**A**) The dsDNA fragments used for the FP assay were 50 nt in length and contain a 10 nt donor DNA region followed by a 40 nt transposon DNA region. The 10 nt donor DNA region is released following the production of a double strand break accompanying strand cleavage. (**B**) This FP assay measures the change in tumbling rate of a population of fluorescently labeled DNA molecules. A fluorescently labeled DNA fragment either free or complexed with Tnp has a particular tumbling rate in solution. This tumbling rate is measured by the change in polarized fluorescence intensity between the time of fluorophore excitation and emission. In this application, the apparent tumbling rate decreases as the number of cleaved donor DNA fragments increases. Thus, any Tnp effector that inhibits strand cleavage without affecting Tnp–DNA binding interactions would in effect increase the observed FP value compared with the value for either the cleaved donor DNA fragments or the free DNA substrate.

metal-bound cleavage intermediates, which would otherwise be difficult to trap. Co-crystallization studies with any compound that affects cleavage in a Tnp–DNA-compound structure could identify the structural basis for the interaction, and one could imagine using these structures in a rational drug design approach, modeling the necessary chemical augmentations required to fit the active site of other superfamily members, such as HIV-1 integrase.

Furthermore, since the transposase/integrase superfamily shares high structural similarities within their catalytic cores, compounds that inhibit Tn*5* Tnp may cross react with other family members (7–9,11). A number of structurally distinct compounds have been recently shown to inhibit both HIV-1 integrase and Tn*5* Tnp activity (B.Ason *et al*., manuscript in preparation). Thus, it remains likely that compounds identified as cleavage inhibitors of Tn*5* Tnp could be useful both as mechanistic probes and in drug discovery for these other family members.

Comparison to other high-throughput assays

Most high-throughput assays targeting this superfamily have focused on HIV-1 integrase (24–29). These assays typically monitor the incorporation of a labeled substrate (the donor) into an immobilized target or the attachment of a labeled target to an immobilized donor. The read-out for these screens focuses on the covalent attachment, or integration, of the donor to the target. Therefore, inhibition could occur at any step of the reaction, such as assembly, 3′ end processing or strand transfer. Thus, it is difficult to distinguish between catalytic and complex assembly inhibitors using these assays. One approach to address this process involves pre-forming

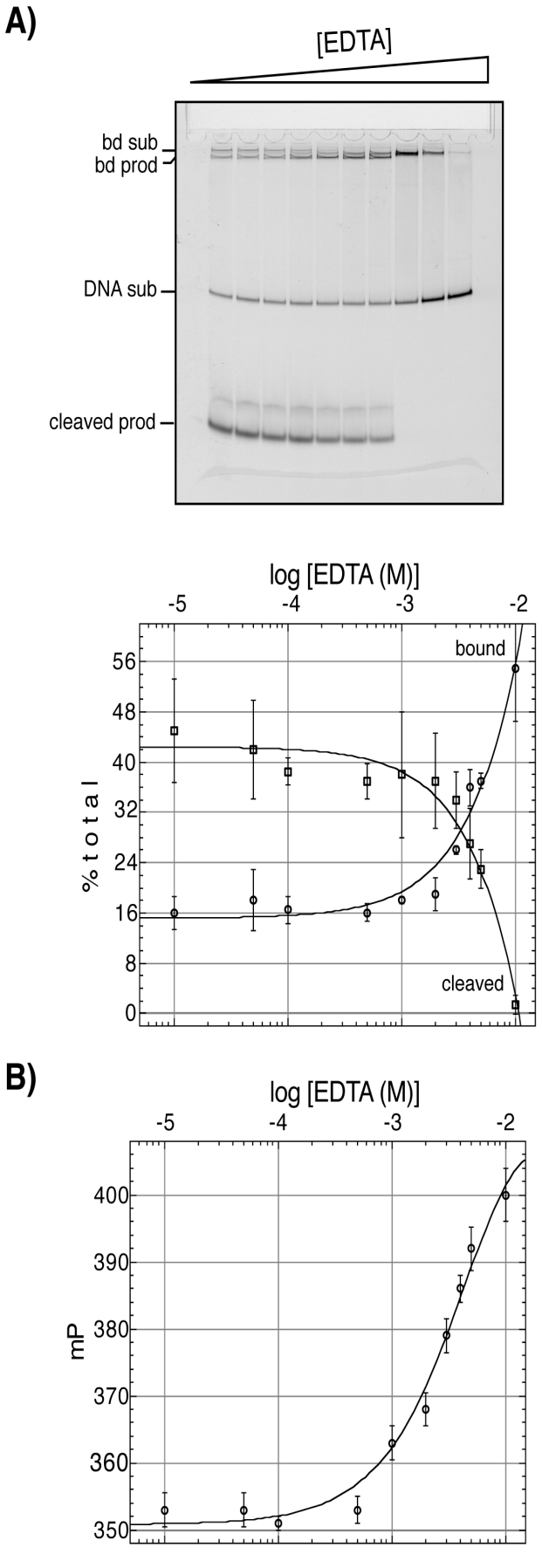

complexes prior to library screening. This has been effective in distinguishing between inhibitors of complex assembly and catalysis in several instances (29,30). However, it remains likely that an inhibitor could disrupt a pre-assembled complex upon addition to the reaction, and since these assays do not measure complex assembly directly, this would be difficult to detect.

Although FP has not been widely reported for assays involving the transposase/integrase superfamily, it has been used extensively in high-throughput screens (31,32). This technique is well established for monitoring protein–DNA binding interactions, and it has also been used to monitor the proteolytic activity for several proteases (33,34). In essence our assay combines these two approaches to identify compounds that are specific for catalysis by coupling both the binding interactions between Tnp and DNA and the physical change in the DNA molecule through DNA cleavage.

The potential drawback for any fluorescence assay used in compound screening is the occurrence of false positives from intrinsically fluorescent compounds. However, most fluorescent compounds can be readily identified as fluorescent, since the signal for reactions containing fluorescent compounds are typically well outside the assay window for our screen (data not shown). Furthermore, confirming a compound's intrinsic fluorescence can easily be determined by monitoring the fluorescence of the compound alone.

CONCLUSIONS

This assay appears to be the first high-throughput assay that selectively targets the DNA cleavage activity catalyzed by the transposase/integrase superfamily of proteins. This assay requires no wash steps and a minimal number of fluid transfer steps. This method is advantageous, since it identifies effectors that are specific for catalysis by eliminating Tnp–DNA binding inhibitors. This, in fact, reduces the number of indirect inhibitors of catalysis that would otherwise be identified as hits. Thus, this method may serve as a valuable aid in the identification of mechanistic probes for the early catalytic steps of this protein superfamily.

Figure 2. A comparison of FP and gel-shift assays indicates that FP is a good measurement of the degree of Tn*5* Tnp-induced strand cleavage. In order to access the relationship between fluorescence polarization and strand cleavage, we compared the degree of strand cleavage that occurred as a function of various EDTA concentrations under the same conditions. Increasing concentrations of EDTA (0, 0.01, 0.05, 0.1, 0.5, 1, 2, 3, 4, 5, 10, 20, 50 M) were used as a mock inhibitor during assay development. (**A**) Strand cleavage reactions were incubated at 37°C for 1.5 h and subsequently loaded onto a 9% native gel for gel-shift assays. The DNA was detected using 5′ fluorescein labeled oligonucleotides. Bd sub indicates the Tnp–DNA substrate complex, bd prod indicates the Tnp–DNA product complex, DNA sub is the substrate, and cleaved prod is the donor DNA cleavage product. The graph represents the percentage of DNA cleavage products compared with the amount of DNA bound by the Tnp per lane from data collect from multiple gel-shift assays. (**B**) Strand cleavage reactions were incubated at 37°C for 1.5 h prior to the FP measurement. The oligonucleotides were labeled with rhodamine green on the 5′ end of the non-transferred strand for these experiments. The graph represents the change in FP signal with increasing concentrations of EDTA. These data indicate that the polarization and strand cleavage data are in good agreement, since the concentration of EDTA that inhibits cleavage is along the same order of magnitude that the polarization begins to increase.

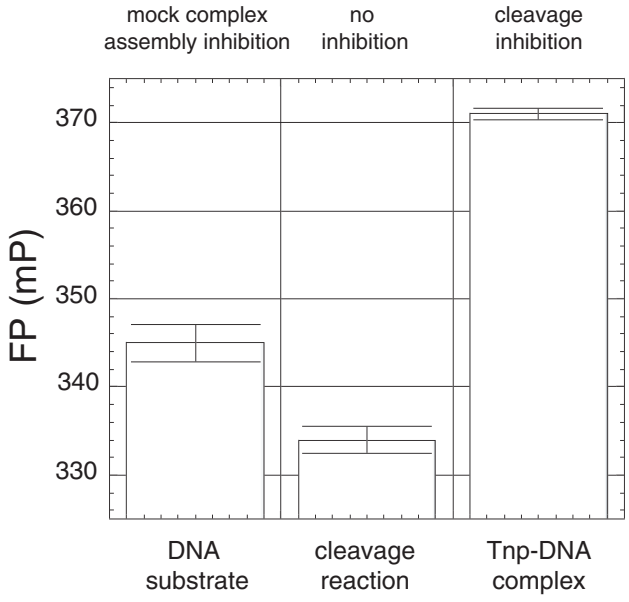

Figure 3. Strand cleavage inhibition is distinguishable from complex assembly inhibition. Tnp complexed with fluorescently labeled DNA exhibits a significantly higher FP value than either the free DNA substrate (mock complex assembly inhibition) or the cleaved donor DNA product (no inhibition). The reactions were performed as originally described in Figure 2 and in Materials and methods. Tnp storage buffer was added to the DNA substrate in place of Tnp for mock complex assembly inhibition. For catalytic inhibition, 10 mM EDTA was added to the cleavage reaction. The reactions were performed in triplicate.

ACKNOWLEDGEMENTS

We thank Allison Balke for her help with some of the preliminary experiments that led to this work and Chris Adams for his critical review of the manuscript. This work was supported by the NIH grant GM50692.

REFERENCES

1. Nancy,L., Craig,R.C., Gellert,M. and Lambowitz,A.M. (2002) *Mobile DNA II*. ASM Press, Washington DC.
2. Bhasin,A., Goryshin,I.Y. and Reznikoff,W.S. (1999) Hairpin formation in Tn5 transposition. *J. Biol. Chem.*, **274**, 37021–37029.
3. Kennedy,A.K., Guhathakurta,A., Kleckner,N. and Haniford,D.B. (1998) Tn10 transposition via a DNA hairpin intermediate. *Cell*, **95**, 125–134.
4. Mizuuchi,K. and Adzuma,K. (1991) Inversion of the phosphate chirality at the target site of Mu DNA strand transfer: evidence for a one-step transesterification mechanism. *Cell*, **66**, 129–140.
5. Engelman,A., Mizuuchi,K. and Craigie,R. (1991) HIV-1 DNA integration: mechanism of viral DNA cleavage and DNA strand transfer. *Cell*, **67**, 1211–1221.
6. Davies,D.R., Braam,L.M., Reznikoff,W.S. and Rayment,I. (1999) The three-dimensional structure of a Tn5 transposase-related protein determined to 2.9-Å resolution. *J. Biol. Chem.*, **274**, 11904–11913.
7. Dyda,F., Hickman,A.B., Jenkins,T.M., Engelman,A., Craigie,R. and Davies,D.R. (1994) Crystal structure of the catalytic domain of HIV-1 integrase: similarity to other polynucleotidyl transferases. *Science*, **266**, 1981–1986.
8. Bujacz,G., Jaskolski,M., Alexandratos,J., Wlodawer,A., Merkel,G., Katz,R.A. and Skalka,A.M. (1995) High-resolution structure of the catalytic domain of avian sarcoma virus integrase. *J. Mol. Biol.*, **253**, 333–346.
9. Rice,P. and Mizuuchi,K. (1995) Structure of the bacteriophage Mu transposase core: a common structural motif for DNA transposition and retroviral integration. *Cell*, **82**, 209–220.
10. Doak,T.G., Doerder,F.P., Jahn,C.L. and Herrick,G. (1994) A proposed superfamily of transposase genes: transposon-like elements in ciliated protozoa and a common ''D35E'' motif. *Proc. Natl Acad. Sci. USA*, **91**, 942–946.
11. Davies,D.R., Goryshin,I.Y., Reznikoff,W.S. and Rayment,I. (2000) Three-dimensional structure of the Tn5 synaptic complex transposition intermediate. *Science*, **289**, 77–85.
12. Johnson,R.C. and Reznikoff,W.S. (1983) DNA sequences at the ends of transposon Tn5 required for transposition. *Nature*, **304**, 280–282.
13. Steiniger-White,M., Bhasin,A., Lovell,S., Rayment,I. and Reznikoff,W.S. (2002) Evidence for ''unseen'' transposase—DNA contacts. *J. Mol. Biol.*, **322**, 971–982.
14. Lovell,S., Goryshin,I.Y., Reznikoff,W.R. and Rayment,I. (2002) Two-metal active site binding of a Tn5 transposase synaptic complex. *Nat. Struct. Biol.*, **9**, 278–281.
15. Ason,B. and Reznikoff,W.S. (2002) Mutational analysis of the base flipping event found in Tn5 transposition. *J. Biol. Chem.*, **277**, 11284–11291.
16. Zhang,J.H., Chung,T.D. and Oldenburg,K.R. (1999) A simple statistical parameter for use in evaluation and validation of high throughput screening assays. *J. Biomol. Screen.*, **4**, 67–73.
17. Asante-Appiah,E., Seeholzer,S.H. and Skalka,A.M. (1998) Structural determinants of metal-induced conformational changes in HIV-1 integrase. *J. Biol. Chem.*, **273**, 35078–35087.
18. Asante-Appiah,E., Skalka,A.M., Seeholzer,S.H., Junop,M.S. and Haniford,D.B. (1999) HIV-1 integrase: structural organization, conformational changes, and catalysis. *Adv. Virus Res.*, **52**, 351–369.
19. Ciubotaru,M., Ptaszek,L.M., Baker,G.A., Baker,S.N., Bright,F.V., Schatz,D.G., Lins,R.D., Straatsma,T.P. and Briggs,J.M. (2003) RAG1-DNA binding in V(D)J recombination. Specificity and DNA-induced conformational changes revealed by fluorescence and CD spectroscopy. *J. Biol. Chem.*, **278**, 5584–5596.
20. Williams,T.L. and Baker,T.A. (2004) Reorganization of the Mu transpososome active sites during a cooperative transition between DNA cleavage and joining. *J. Biol. Chem.*, **279**, 5135–5145.
21. Allingham,J.S. and Haniford,D.B. (2002) Mechanisms of metal ion action in Tn10 transposition. *J. Mol. Biol.*, **319**, 53–65.
22. Mundy,C.L., Patenge,N., Matthews,A.G. and Oettinger,M.A. (2002) Assembly of the RAG1/RAG2 synaptic complex. *Mol. Cell Biol.*, **22**, 69–77.
23. Hwang,Y., Rhodes,D. and Bushman,F. (2000) Rapid microtiter assays for poxvirus topoisomerase, mammalian type IB topoisomerase and HIV-1 integrase: application to inhibitor isolation. *Nucleic Acids Res.*, **28**, 4884–4892.
24. Hazuda,D.J., Felock,P., Witmer,M., Wolfe,A., Stillmock,K., Grobler,J.A., Espeseth,A., Gabryelski,L., Schleif,W., Blau,C. *et al.* (2000) Inhibitors of strand transfer that prevent integration and inhibit HIV-1 replication in cells. *Science*, **287**, 646–650.
25. Hazuda,D.J., Hastings,J.C., Wolfe,A.L. and Emini,E.A. (1994) A novel assay for the DNA strand-transfer reaction of HIV-1 integrase. *Nucleic Acids Res.*, **22**, 1121–1122.
26. Craigie,R., Mizuuchi,K., Bushman,F.D. and Engelman,A. (1991) A rapid *in vitro* assay for HIV DNA integration. *Nucleic Acids Res.*, **19**, 2729–2734.
27. Vink,C., Banks,M., Bethell,R. and Plasterk,R.H. (1994) A high-throughput, non-radioactive microtiter plate assay for activity of the human immunodeficiency virus integrase protein. *Nucleic Acids Res.*, **22**, 2176–2177.
28. Hazuda,D., Felock,P.J., Hastings,J.C., Pramanik,B. and Wolfe,A.L. (1997) Discovery and analysis of inhibitors of the human immunodeficiency integrase. *Drug Des. Discov.*, **15**, 17–24.
29. Hazuda,D.J., Felock,P.J., Hastings,J.C., Pramanik,B. and Wolfe,A.L. (1997) Differential divalent cation requirements uncouple the assembly and catalytic reactions of human immunodeficiency virus type 1 integrase. *J. Virol.*, **71**, 7005–7011.
30. Owicki,J.C. (2000) Fluorescence polarization and anisotropy in high throughput screening: perspectives and primer. *J. Biomol. Screen.*, **5**, 297–306.

31. Burke,T.J., Loniello,K.R., Beebe,J.A. and Ervin,K.M. (2003) Development and application of fluorescence polarization assays in drug discovery. *Comb. Chem. High Throughput. Screen.*, **6**, 183–194.
32. Lundblad,J.R., Laurance,M. and Goodman,R.H. (1996) Fluorescence polarization analysis of protein–DNA and protein–protein interactions. *Mol. Endocrinol.*, **10**, 607–612.
33. Levine,L.M., Michener,M.L., Toth,M.V. and Holwerda,B.C. (1997) Measurement of specific protease activity utilizing fluorescence polarization. *Anal. Biochem.*, **247**, 83–88.
34. Artico,M., Di Santo,R., Costi,R., Novellino,E., Greco,G., Massa,S., Tramontano,E., Marongiu,M.E., De Montis,A. and La Colla,P. (1998) Geometrically and conformationally restrained cinnamoyl compounds as inhibitors of HIV-1 integrase: synthesis, biological evaluation, and molecular modeling. *J. Med. Chem.*, **41**, 3948–3960.